(Reprinted from Nature, Vol. 257, No. 5521, pp. 28–32, September 4, 1975)

Please don't remove

Three-dimensional model of purple membrane obtained by electron microscopy

R. Henderson & P. N. T. Unwin

MRC Laboratory of Molecular Biology, Hills Road, Cambridge CB2 2QH, UK

A 7-Å resolution map of the purple membrane has been obtained by electron microscopy of tilted, unstained specimens. The protein in the membrane contains seven, closely packed, α-helical segments which extend roughly perpendicular to the plane of the membrane for most of its width. Lipid bilayer regions fill the spaces between the protein molecules.

THE purple membrane is a specialised part of the cell membrane of *Halobacterium halobium*[1]. Oesterhelt and Stoeckenius[2] have shown that it functions *in vivo* as a light-driven hydrogen ion pump involved in photosynthesis. It contains identical protein molecules of molecular weight 26,000, which make up 75% of the total mass, and lipid which makes up the remaining 25% (ref. 3). Retinal, covalently linked to each protein molecule in a 1:1 ratio is responsible for the characteristic purple colour[3]. These components together form an extremely regular two-dimensional array[4].

We have studied the purple membrane by electron microscopy using a method for determining the projected structures of unstained crystalline specimens[5]. By applying the method to tilted specimens, and using the principles put forward by De Rosier and Klug[6] for the combination of such two-dimensional views, we have obtained a three-dimensional map of the membrane at 7 Å resolution. The map reveals the location of the protein and lipid components, the arrangement of the polypeptide chains within each protein molecule, and the relationship of the protein molecules in the lattice.

Electron microscopy and diffraction

The purple membrane was prepared under normal conditions from cultures of *H. halobium*[3] and applied to the microscope grid in the presence of 0.5% glucose. The purified membranes are mostly oval sheets up to 1.0 μm in diameter and about 45 Å thick[4,7]. The array of molecules making up these sheets is accurately described[7] as an almost perfect crystal of space group P3 ($a = 62$ Å) with a thickness of one unit cell only in the direction of the c axis. A single membrane thus contains up to 40,000 unit cells; that is 120,000 protein molecules (three per unit cell).

These large periodic arrays from which electron diffraction patterns and defocused bright field micrographs are recorded[5] enable us to overcome the principal problem normally associated with high resolution electron microscopy of unstained biological materials; that is, sensitivity to electron damage[8]. Only a small number of electrons can pass through each unit cell before it is destroyed, but because of the large number of unit cells, the information in the diffraction patterns and micrographs is sufficient to provide a picture of the average unit cell. The micrographs recorded with such low doses of electrons appear featureless, since the statistical fluctuation in the number of electrons striking the plate is large compared with the weak phase contrast (< 1%) produced by defocusing.

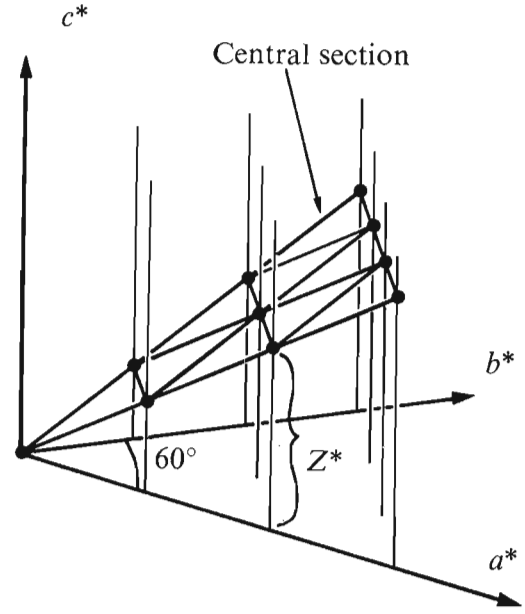

Fig. 1 Part of the three-dimensional reciprocal lattice showing the geometry of the lattice lines in the hexagonal space group P3. a^*, b^* and c^* are the reciprocal lattice vectors. a^* and b^* lie in, and c^* is perpendicular to the plane of the membrane. A central section which is perpendicular to the incident electron beam has been drawn through the lattice. The intersection of this central section with the reciprocal lattice is determined by the angle of tilt and the axis about which the membrane is tilted. Individual diffraction patterns and micrographs provide the amplitudes and phases in this section at the points shown. z^* represents the coordinate along the c^* direction of one of the points. The angle of tilt was measured to within 2° for each of the specially modified, tilted specimen holders, and the direction of the tilt axis on the photographic plate was established during operation of the microscope. However, estimates based on the geometry of the spacings of the lattice points (for high tilt angles), the variation of the degree of underfocus across the plate (for low tilt angles), and least squares refinement against data obtained at high tilt angles (for diffraction patterns) provided more accurate figures which were used in the calculation. The accuracy of measurement of both the amplitudes and phases depended on having sharp lattice lines. We therefore took care to ensure that, on the microscope grid, the membranes remained coherently ordered and flat to within 1/5°.

As a result, analysis of each micrograph by densitometry and computer processing[5] is required to combine the information from individual unit cells.

Solution of the three-dimensional structure of the purple membrane requires the determination of the amplitudes and phases in three dimensions of the Fourier terms into which it can be analysed. The diffraction pattern or Fourier transform of the membrane is not a three-dimensional lattice of points as is the case with a normal crystal, but since it is only one unit cell thick, a two-dimensional lattice of lines which are continuous in the direction of c^* (that is perpendicular to the membrane). A single electron diffraction experiment therefore

gives rise to a two-dimensional pattern of spots which correspond in their intensities to the square of the amplitudes of the transform along a central section through the three dimensional transform of the membrane (Fig. 1). Similarly, an electron micrograph contains information about the phases (and about the amplitudes, but less accurately than does the diffraction pattern) in the central section. Previously[5], we were able to determine the projected structures of both the purple membrane and thin catalase crystals from the amplitudes (obtained by electron diffraction) and phases (by Fourier analysis of micrographs) along the single central section through the transform parallel to the plane of the object.

Here, we have collected data similar to those obtained previously but from 15 diffraction patterns and 18 micrographs (actually pairs of micrographs, see ref. 5) of membranes tilted at angles from 0° to 57° to the incident electron beam, to determine the amplitudes and phases at a number of points along each of the lattice lines. These data provided estimates of the continuous variation of the transform along the lines. By sampling the continuous curves at appropriate intervals, it was then possible to calculate the structure as if for a three-dimensional crystal with some arbitrary *c*-axis dimension greater than the membrane thickness. This method of combining two-dimensional images was proposed originally by De Rosier and Klug[6] for a general object, although in this case we have made use of electron diffraction patterns as well.

The diffraction patterns provided 1,800 independent intensity measurements which were combined to give continuous curves, such as those shown in Fig. 2, for each of the 36 crystallographically independent lattice lines out to a resolution of 7 Å. Because of the distribution of intensity in the transform[7], due to real features in the structure, very little diffracted intensity (none greater than 1/50th of the strongest intensity) occurred at values of z^* greater than 0.08 $Å^{-1}$ for any lattice line.

With the electron micrographs compensation for the effects of defocus was rather more complicated than in the case of untilted specimens[5]. Since the membranes we studied were at least 5,000 Å in diameter, different parts of the membrane in a tilted specimen were situated at significantly different distances from the objective lens. As a result, the phase contrast transfer function, which depends on the degree of underfocus of this lens, varied across the image. The correction of the contrast of the image could not be made after transforming the image by altering the phases of the Fourier components of the image, as was done previously, but instead had to be carried out at an earlier stage, so that different parts of the image where the contrast is positive or negative could be made to combine constructively, and thereby yield, on transformation, the correct

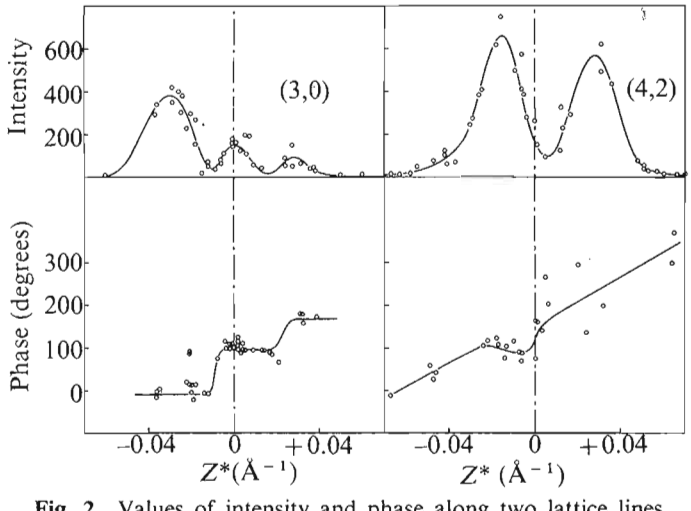

Fig. 2 Values of intensity and phase along two lattice lines, obtained respectively from the diffraction patterns and images using the geometry shown in Fig. 1. Smooth curves were drawn through the points to give reliable intensities and phases at suitably fine sampling intervals (0.01 $Å^{-1}$) in z^*. These values were used to compute the three-dimensional structure.

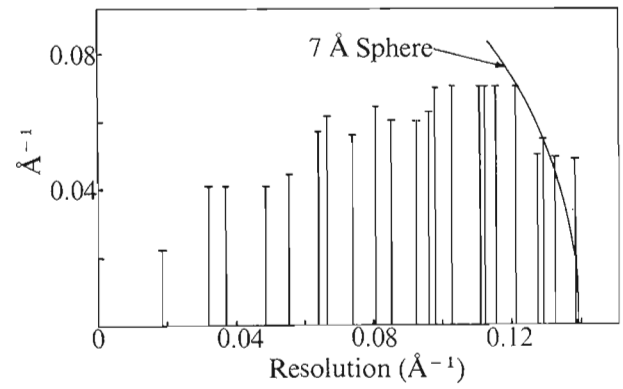

Fig. 3 Schematic diagram showing the region of reciprocal space contributing to the three-dimensional Fourier map. Part of the boundary of the 7 Å sphere is indicated. The region shown, which includes 63% of the total volume of this sphere, includes almost all the strong diffraction peaks to 7 Å, with the principal exception of the axial (0,0) lattice line (but see text).

phases for the object. This procedure was conveniently carried out between the execution of the first and second dimensions of the Fourier transformation having ensured that the images were densitometered parallel to the tilt axis. The contrast along each scan line could then be corrected by multiplying the one-dimensionally transformed data by the contrast transfer function, $-2\sin\chi$ (see ref. 5) for each reflection, so that the computed phases had the correct sign for the object, and gave the maximum signal-to-noise ratio. The phases were then combined image by image after refining the phase origin of each image so that the best agreement of its phases with all previously accumulated phases was obtained. By starting with the untilted data with the phase origin at one of the threefold positions, and adding the phases from images with smaller tilt angles first, the maximum accuracy in combining the phases was ensured. This procedure also meant that the phase origin for the combined three-dimensional data ended roughly in the middle of the membrane on one of the threefold axes. The average phase error in a single measurement estimated from the differences between those of the 1,000 independently recorded phases having similar values of z^* was less than 20°, as found previously[5]. As with the intensity data, continuous curves could be drawn through these phase measurements (Fig. 2).

The intensity and phase curves were sampled at intervals of 0.01 $Å^{-1}$ to provide Fourier terms from which to calculate the three-dimensional map. This sampling interval is more than sufficiently fine to ensure an accurate representation of a structure only 45 Å thick.

Three-dimensional potential map

The map (Fig. 4) was a Fourier synthesis of 365 crystallographically independent terms which extended to a resolution of 7 Å in the plane of the membrane, but which included only terms with spacings greater than 14 Å perpendicular to it. There were two reasons for the asymmetrical distribution of Fourier terms. First, the distribution of intensity in the transform of the membrane is such that the diffraction beyond spacings of 7 Å in the plane of the membrane, and about 20 Å perpendicular to it, is weak and therefore difficult to measure with the limited total diffraction available from membranes only 1 μm in diameter. The average intensity in these regions by X-ray diffraction[7] is 7–10 times lower than the in-plane diffraction near 10 Å, and by electron diffraction we find no intensity greater than 1/50th of the strongest diffraction at values of z^* greater than 0.080 $Å^{-1}$. Second, the use of tilt angles up to some limiting angle, in this case 57°, meant that a conical region of reciprocal space was unmeasured. The volume of reciprocal space finally included is shown schematically in Fig. 3. Although a considerable volume of the 7 Å sphere is missing (37%) the effect of its inclusion in the map would be

very small since the X-ray diffraction pattern indicates that the amplitudes of the Fourier components in the missing regions are small. Therefore, since the map includes all the strong terms present to 7 Å resolution, it provides an accurate representation of the dominating features of the structure to this resolution.

As a further check on the effect of leaving out some of the near axial reflections, a second map was calculated which included the profile diffraction determined by X rays. The amplitudes were obtained from the published X-ray profile

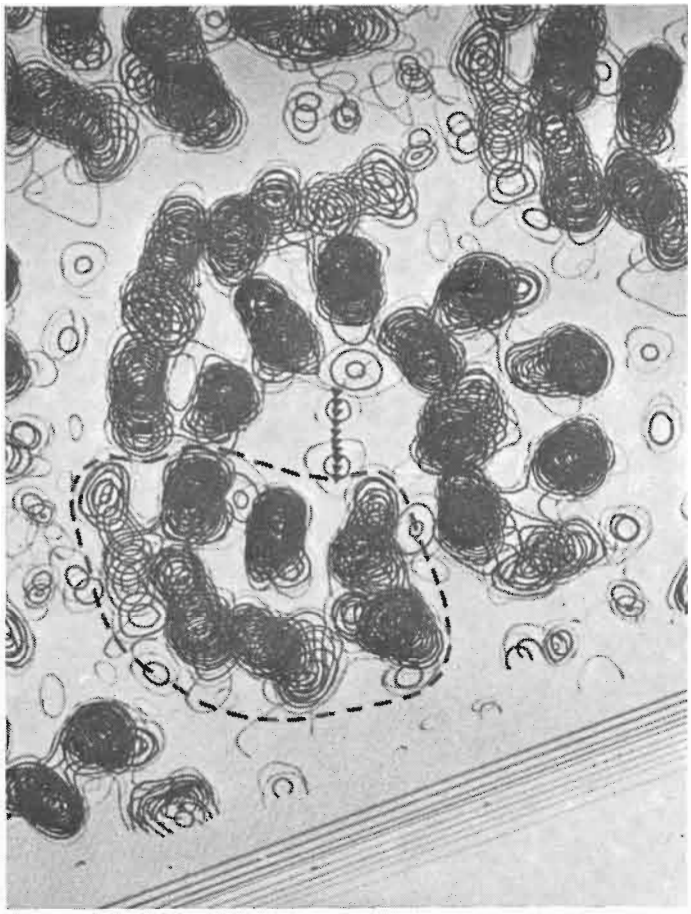

Fig. 4 Part of the three-dimensional potential map showing a region 50 Å thick spanning the membrane. The sections above and below this region contain no features higher than one contour level. The absolute hand is determined by the known direction of specimen tilt. The view shows protein molecules grouped around one of the threefold axes. The probable boundary of one of them is indicated by the broken line. The angle of view is such that the α helices furthest from the threefold axis partly overlap in the protein molecule outlined, but are seen almost end-on in the one on the right.

of Blaurock and Stoeckenius[4] by sampling at 0.01 $Å^{-1}$ intervals, and scaled to our data by comparing the profile intensity with that of the (1,1) ring in an unoriented X-ray powder pattern. The phases were assumed to be those of a symmetrical membrane[4] with the origin in the middle. The inclusion of the Fourier terms out to 0.05 $Å^{-1}$ made little difference to the map but, as would be expected, slightly raised the overall level of the contours on each side of the membrane (by about one contour level). The axial (0,0) line is by far the strongest region not included in our map, so clearly the effect of excluding the remaining unmeasured volume of reciprocal space is small.

Since the amplitudes and phases used to calculate the present map are derived from the scattering of electrons, the physical quantity which it represents is, strictly, the electrical potential inside the membrane. At this resolution, however, the potential is roughly proportional both to the electron density, as would be found for instance by X-ray analysis, and to the atomic number. High density features therefore correspond to the presence of denser groupings of atoms.

Structure of the membrane

The appearance of the map is dominated by numerous rod-shaped features aligned perpendicular to the plane of the membrane. There are seven rods in each asymmetric unit of the crystal and they are packed 10–12 Å apart. Adjacent rods are slightly inclined to one another at various angles from 0° to 20° and they are all roughly 35–40 Å long. In view of the existence[7,9] in the X-ray diffraction pattern of strong axial reflections at 1.5 Å and 5 Å which are characteristic of the α-helix, there is little doubt that the seven rod-shaped features in the map are α-helices which extend perpendicular to the membrane for most of its width. Since the protein has a molecular weight of 26,000 (ref. 3), it follows that the α-helices make up 70–80% of the polypeptide. The connectivity of the helices, however, cannot be discerned unambiguously at this resolution.

The tentative boundary of an individual protein molecule indicated in Fig. 4 is the one most likely to be correct since it surrounds regions of the protein with maximum connectivity and it is this part of the map which we have used to make the model shown in Fig. 5. The overall dimensions of the protein in our model are $25 \times 35 \times 45$ Å, with the longest dimension perpendicular to the plane of the membrane and parallel to the helices. The three protein molecules which are most intimately in contact are grouped round the threefold axis in an interesting manner. Three of the seven α helices in each

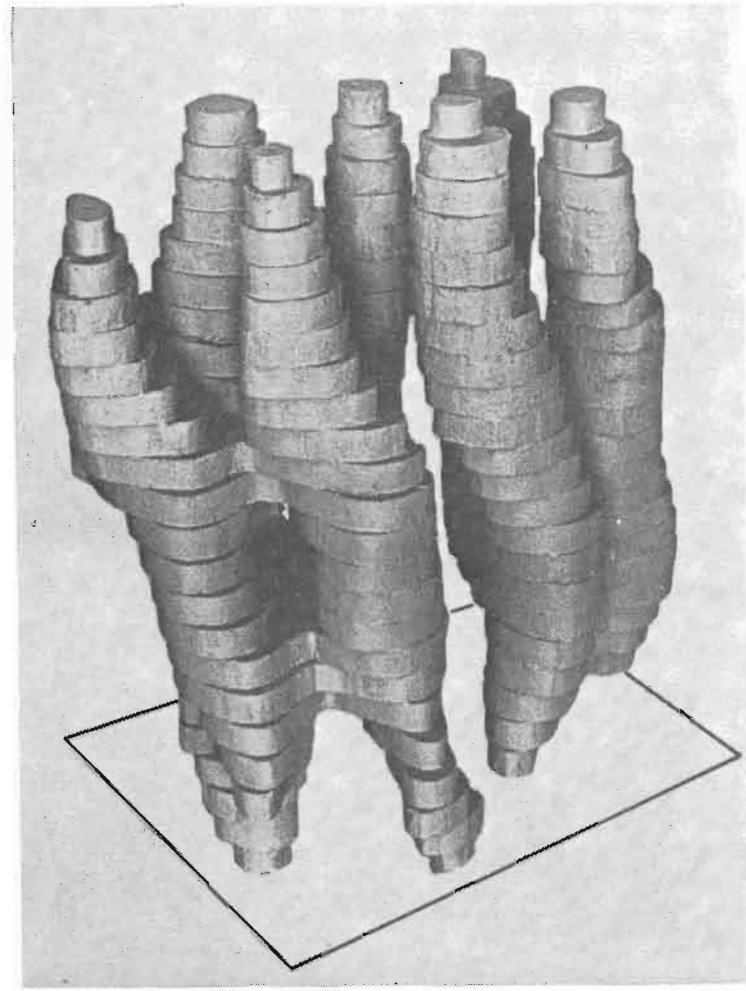

Fig. 5 A model of a single protein molecule in the purple membrane, viewed roughly parallel to the plane of the membrane. The top and bottom of the model correspond to the parts of the protein in contact with the solvent, the rest being in contact with lipid. The most strongly tilted α helices are in the foreground.

protein molecule are nearer the centre of the group giving an inner ring of nine helices which are all 10 Å (±1) apart and in contact with one another. The other four helices in each protein combine to make an outer ring of twelve which surround the inner nine. The outer helices are all slightly more inclined to the perpendicular than the inner ones, and are not all in contact. The three most strongly tilted of these helices were not resolved in projection[5], since they partly superimpose when viewed perpendicular to the plane of the membrane. The direction of tilting of the outer helices is consistent with the interlocking of the amino acid side chains from adjacent helices—that is the structure is a left-handed supercoil, as expected for a right-handed α helix[10].

In the space in the middle of the ring of nine helices, we presume that a small number of lipid molecules is arranged in the classical bilayer configuration. This space has a diameter of about 20 Å; it is not a hole filled with solvent since a difference map using X-ray intensities from wet versus dry membranes is featureless. Evidence obtained from another difference map shows that UO_2^{+2} ions can bind to this region of the membrane, again suggesting that the space is filled with lipid. Similar arguments that a lipid bilayer must be present apply to the rather even density regions which make up the remainder of the membrane structure, filling up the space between the clusters of three protein molecules.

At this resolution we cannot detect the covalently linked retinal molecule, which is thought, from measurements of the dichroism at 560 nM in oriented specimens[4], to be aligned parallel to the plane of the membrane—that is, perpendicular to the helices.

The structure of the purple membrane protein and the way it combines with lipid to form a two-dimensional mosaic in which the protein and lipid pack neatly side by side, each with a thickness of about 45 Å, gives experimental support to recent concepts[11,12] of membrane structure based on less direct evidence. In particular, the protein is globular, is almost certainly exposed on both sides of the membrane, and is surrounded by lipids which are arranged in separate areas with a bilayer configuration. The purple membrane thus seems to provide a simple example of an 'intrinsic' membrane protein, a class of structure to which many molecular pumps and channels must belong. We would not be surprised if the simple arrangement of helices found here also occurs in some of these other intrinsic membrane proteins.

A full account of this work will be published elsewhere. We thank Dr J. Pilkington and the Royal Greenwich Observatory for help with and facilities for the densitometry of the micrographs, Chris Raeburn for modifying the specimen holders and Drs L. Amos, T. Horsnell, R. Ladner and T. Takano for computer programs. We also thank our colleagues in this laboratory, particularly Dr A. Klug, for comments on the manuscript.

Received June 24; accepted July 29, 1975.

1 Stoeckenius, W., and Kunau, W. H., *J. Cell Biol.*, **38**, 337–357 (1968).
2 Oesterhelt, D., and Stoeckenius, W., *Proc. natn. Acad. Sci. U.S.A.*, **70**, 2853–2857 (1973).
3 Oesterhelt, D., and Stoeckenius, W., *Nature new Biol.*, **233**, 149–152 (1971).
4 Blaurock, A. E., and Stoeckenius, W., *Nature new Biol.*, **233**, 152–155 (1971).
5 Unwin, P. N. T., and Henderson, R., *J. molec. Biol.*, **94**, 425–440 (1975).
6 De Rosier, D. J., and Klug, A., *Nature*, **217**, 130–134 (1968).
7 Henderson, R., *J. molec. Biol.*, **93**, 123–138 (1975).
8 Glaeser, R. M., in *Physical Aspects of Electron Microscopy and Microbeam Analysis* (edit. by Siegel, B., and Beaman, D. R.), 205 (Wiley, New York, 1975).
9 Blaurock, A. E., *J. molec. Biol.*, **93**, 139–158 (1975).
10 Crick, F. H. C., *Acta Cryst.*, **6**, 689–697 (1953).
11 Singer, S. J., and Nicholson, G. L., *Science*, **175**, 720–731 (1972).
12 Bretscher, M. S., *Science*, **181**, 622–629 (1973).

Printed in Great Britain by Henry Ling Ltd., at the Dorset Press, Dorchester, Dorset